Multidiszciplináris Tudományok, 15. kötet, 1. sz. (2025) pp. 37–53. **https://doi.org/10.35925/j.multi.2025.1.4**

FATIGUE CRACK PROPAGATION IN S1100M AND S1300Q STRUCTURAL STEELS AND THEIR WELDED JOINTS

Judit Kovács
assistant research fellow, Institute of Materials Science and Technology
3515 Miskolc-Egyetemváros, e-mail: judit.kovacs@uni-miskolc.hu

János Lukács
full professor, Institute of Materials Science and Technology
3515 Miskolc-Egyetemváros, e-mail: janos.lukacs@uni-miskolc.hu

Abstract
Nowadays, in case of thick plates, materials with a yield strength of 1100 MPa or 1300 MPa are available, depending on the production method. However, the resistance of these materials to fatigue crack propagation (FCP) is still a question. Thus, in the present research work, tests are presented on the fatigue crack propagation resistance of S1100M and S1300Q base materials and their welded joints. For the welded joints two different types of filler materials from different strength categories were used, so these were also compared in the terms of fatigue crack propagation resistance. The results show a significant difference between cracks propagating in the rolling direction and in the thickness direction. However, for the two different filler metals, the resistance of the welded joints to fatigue crack propagation is considered to be the same. For S1100M, the fatigue fracture toughness of welded joints typically exceeds that of the base material. In the case of S1300Q, there is no significant difference between the fatigue fracture toughness of the base material and that of the welded joints.

Keywords: *high strength steel, fatigue crack propagation, gas metal arc welding*

1. Introduction

Steel is one of the most important structural material worldwide, and the development of structural steels has global impacts (Lahtinen et al., 2019), (Raabe, 2023). With the right chemical composition, rolling conditions and heat treatment, thick plates with yield strengths up to 1300 MPa can be produced. These steel grades are usually produced by quenching and tempering, and its microstructure will be martensitic (Jha et al., 2012), (Shi et al., 2012). Another production method for high strength steels is thermomechanical rolling, which nowadays allows the production of thick plates with yield strengths up to 1100 MPa. High strength steels are mainly used in heavy-duty components and construction cranes, but despite being available for many years, those are less frequently used (Weglowski et al., 2013), (Weglowski et al., 2014). One reason for this may be that the relevant standards do not contain specifications for steels with yield strengths above 1000 MPa. The use of such steels, especially in welded structures, therefore, requires careful design and extensive testing (Weglowski et al., 2013), (Tümer et al., 2021), (Chen et al., 2023).

For structures (mainly welded structures) subjected to cyclic loading, it is important to investigate the fatigue crack growth rate. Crack growth can be divided into three phases: slow growth, stable growth, and unstable crack propagation. Once the crack enters the unstable range, the damage is irreversible. Fatigue crack propagation is highly dependent on the structural properties of the material and the test conditions. Microstructural characteristics influence the crack propagation path and velocity, and hence the fracture morphology. Since different materials have different microstructure and mechanical properties, and therefore different crack propagation behavior, before application this should also be investigated (Yu et al., 2011), (Zhang et al., 2022), (Li et al., 2022).

In all cases, the final aim of the tests and the analyses is to help assess the integrity of welded structures made of these steels (Lukács et al., 2012). There are several aspects of structural integrity (Koncsik, 2021; Koncsik, 2022) and its reliable application requires statistically based materials characteristics. Reliability can be further increased by taking into account the effects of the main factors (e. g. the manufacturing process of the base material, production processes of the structural element or structure, technological parameters of the processes, post process treatments) influencing the materials characteristics (Lukács et al., 2012).

In the present research work the resistance to fatigue crack propagation was examined for the selected S1100M and S1300Q base materials and their welded joints. As the filler material also influences the fatigue crack propagation behavior, the effect of the chosen filler materials that belongs to different strength categories were also examined.

2. Materials and methods

One of the investigated materials was Alform 1100M x-treme (S1100M) produced by Voestalpine and the other was a structural steel corresponding to material grade S1300Q, for which no data sheet was available, so its mechanical properties had to be determined and a chemical analysis had to be performed. The mechanical properties of the investigated steels are given in *Table 1* and their chemical composition in *Table 2* and *Table 3*. In these tables, the data for the S1100M material are based on the datasheet, while for the S1300Q the values were determined at the University of Miskolc.

Table 1. *Thicknesses and mechanical properties of the investigated steels*

Base material	Thickness [mm]	Vickers hardness HV10	$R_{p0.2}$ [MPa]	R_m [MPa]	A [%]	CVN at –40 °C [J]
S1100M	15	394	1193	1221	11.6	88
S1300Q	10	468	1300	1560	12.0	78

Table 2. *Chemical composition of the S1100M base material [weight%]*

C	Si	Mn	P	S	Cr	Cu	Ni	Mo	V	Ti	Al	Nb	B
0.13	0.32	1.62	0.009	0.0015	0.63	0.047	0.32	0.62	0.066	0.011	0.035	0.037	0.0014

Table 3. *Chemical composition of the S1300Q base material [weight%]*

C	Si	Mn	P	S	Cr	Cu	Ni	Mo	V	Ti	Al	Nb	Zr
0.23	0.45	1.86	0.012	0.001	0.85	0.093	2.43	0.36	0.03	0.002	0.063	<0.001	<0.001

For the S1100M material, the carbon equivalent value on the data sheet is CE = 0.68%, and for the S1300Q steel, the carbon equivalent value was calculated on the basis of the measured chemical composition is CE = 0.956%.

Optical microscopic images of the investigated steels in delivery condition at N = 200× magnification are presented in *Figure 1*. The image of S1100M shows the typical fine-grained microstructure of thermomechanically rolled steels, while the image of S1300Q shows the typical tempered martensitic microstructure of the ultra-high strength steels. The specimens were etched with Nital (3% HNO_3).

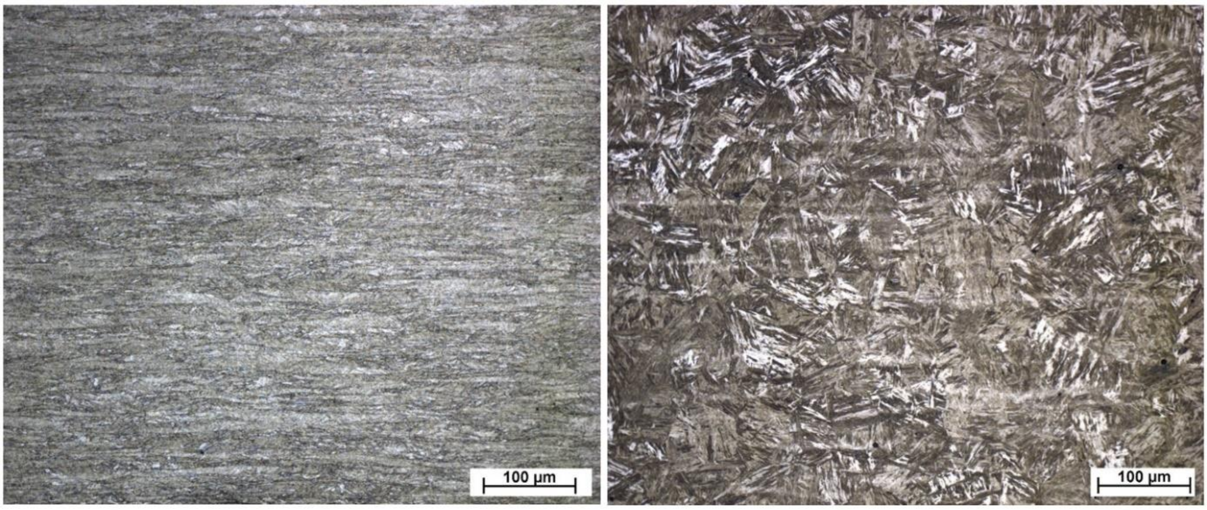

a, b,

Figure 1. *Microstructure of the base materials, N = 200×, etching: 3% HNO_3 (a, S1100M; b, S1300Q)*

Welded joints were prepared on the investigated high strength steels with two different strength grades of filler materials, Böhler Union X96 (Ø 1.2 mm) and Böhler alform 1100 L-MC (Ø 1.2 mm). The mechanical properties of the filler materials are given in *Table 4* and their chemical composition in *Table 5*.

Table 4. *Mechanical properties of the filler materials*

Filler material	R_{eL} or $R_{p0,2}$ [MPa]	R_m [MPa]	A [%]	CVN at –40 °C [J]
Böhler Union X96	≥930	≥980	≥14	≥47
Böhler alform 1100 L-MC	≥1100	1140–1250	≥10	≥27

Table 5. *Chemical composition of the filler materials [weight%]*

Filler material	C	Si	Mn	P	S	Cr	Mo	Ni	V
Böhler Union X96*	0.1	0.8	1.94	0.015	0.011	0.52	0.53	2.28	<0.01
Böhler alform 1100 L-MC	0.08	0.46	1.54	0.01	0.007	0.64	0.52	2.73	0.22

* Cu = 0.06; Ti = 0.06; Al < 0.01; Zr < 0.01

The welding parameters were determined according to the chosen $t_{8/5}$ cooling time (which was selected on the basis of previous experiments and literature research). The welding parameters determined for the two base materials are given in *Table 6* and *Table 7*.

Table 6. *Welding parameters in case of S1100M steel*

Welding pass number	Welding current [A]	Welding voltage [V]	Welding speed [cm/min]	$t_{8/5}$ cooling time [s]	Heat input [J/mm]
1	180	19.1	24	5	688
2	190	19.7	27		666
3–4	260	25.1	50		624
5–8	280	28.7	61		632

Table 7. *Welding parameters in case of S1300Q steel*

Welding pass number	Welding current [A]	Welding voltage [V]	Welding speed [cm/min]	$t_{8/5}$ cooling time [s]	Heat input [J/mm]
1–2	180	19.1	31	5	562
3–4	240	22.7	53		493

The process chosen to produce the joints was gas metal arc welding, using a Daihen WB-P500L power source. The 350 mm × 150 mm × 10/15 mm plates with X-groove were welded in PA position. A schematic illustration of the X-groove and the welding passes are shown in *Figure 2*.

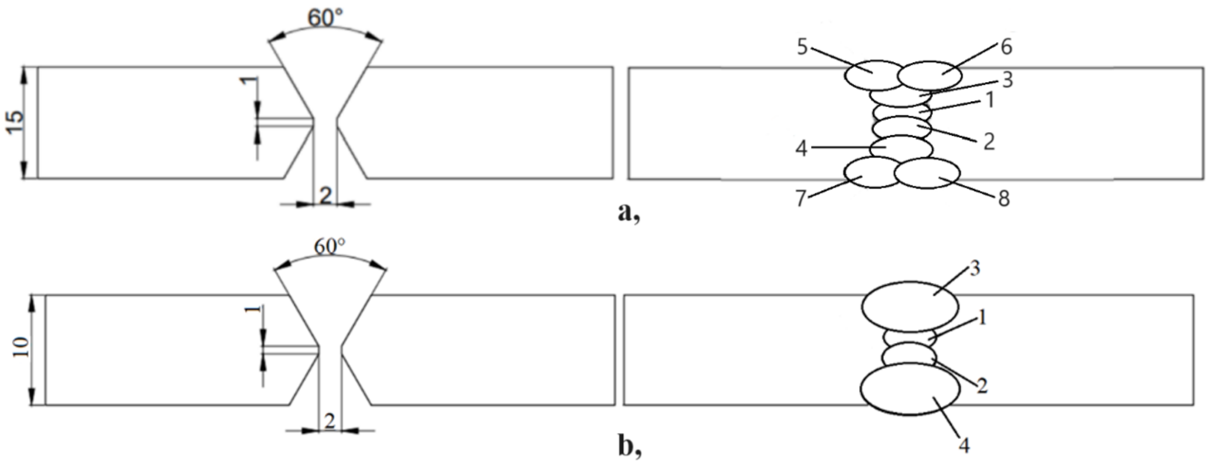

Figure 2. *Schematic illustration of the X-groove and the welding passes (a, S1100M; b, S1300Q)*

To ensure a uniform welding speed and weld seam (except for the first pass), the torch was moved by an ESAB B5001 welding tractor. The applied preheating temperature was 100 °C, taking into account previous own experiments and literature recommendations (Weglowski et al., 2014), (Voestalpine, 2024), and the interpass temperature was approximately 130 °C. Shielding gas mixture of 80% Ar + 20% CO_2 (M21) with a flow rate of 18 l/min was used.

3. Experiment

The fatigue crack propagation tests were performed using an MTS universal electro-hydraulic material testing system (MTS 312). In order to evaluate the resistance to crack propagation, three-point bending specimens (TPB) were prepared from the tested base materials and their welded joints with different filler materials. From the welded joints, the specimens were prepared as shown in *Figure 3*.

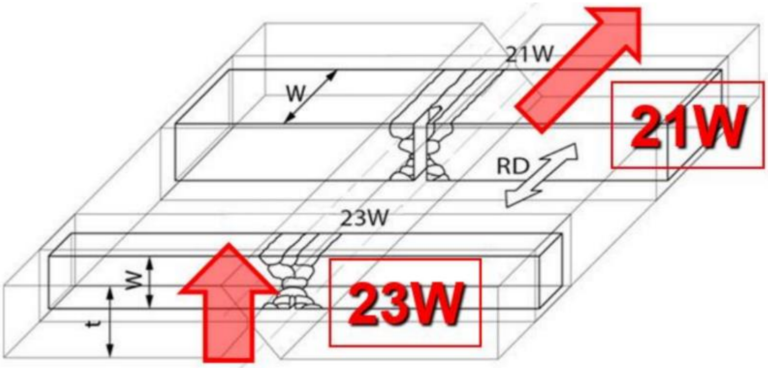

Figure 3. *Design of three-point bending specimens from welded joints, with marked notch directions* (Mobark, 2020)

Specimens with T-L and T-S orientations were prepared from the two base materials, while specimens with 21 and 23 orientations (ASTM E1823-21, 2021) were prepared from the welded joints. The location of the notches for welded joints is illustrated in *Figure 4* and *Figure 5*.

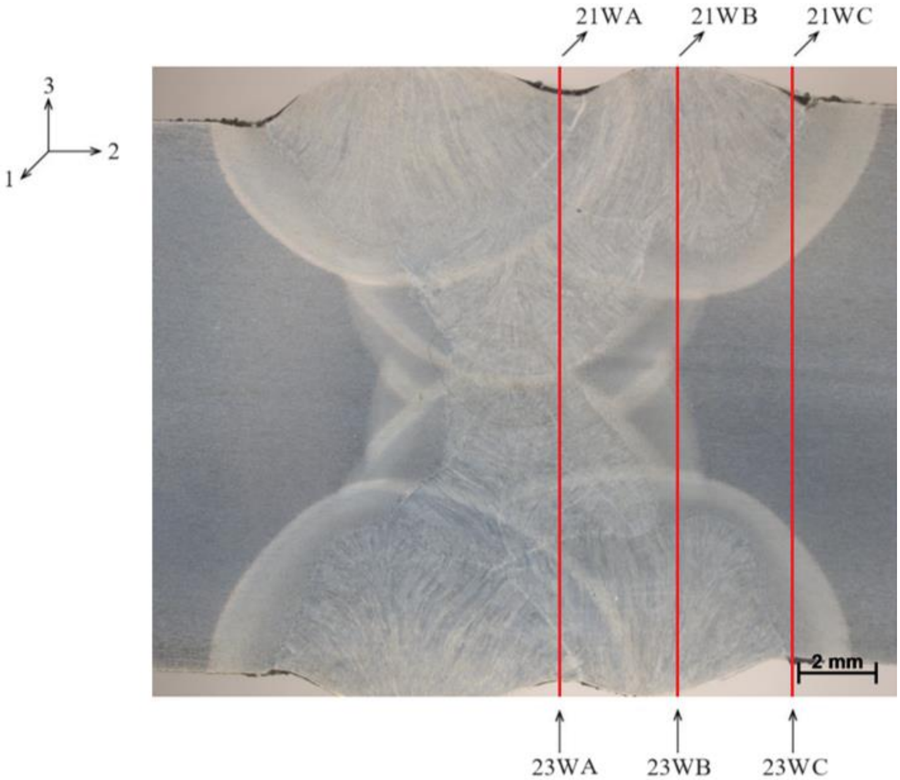

Figure 4. *Notch orientation of TPB specimens used for fatigue crack propagation tests for welded joints of S1100M*

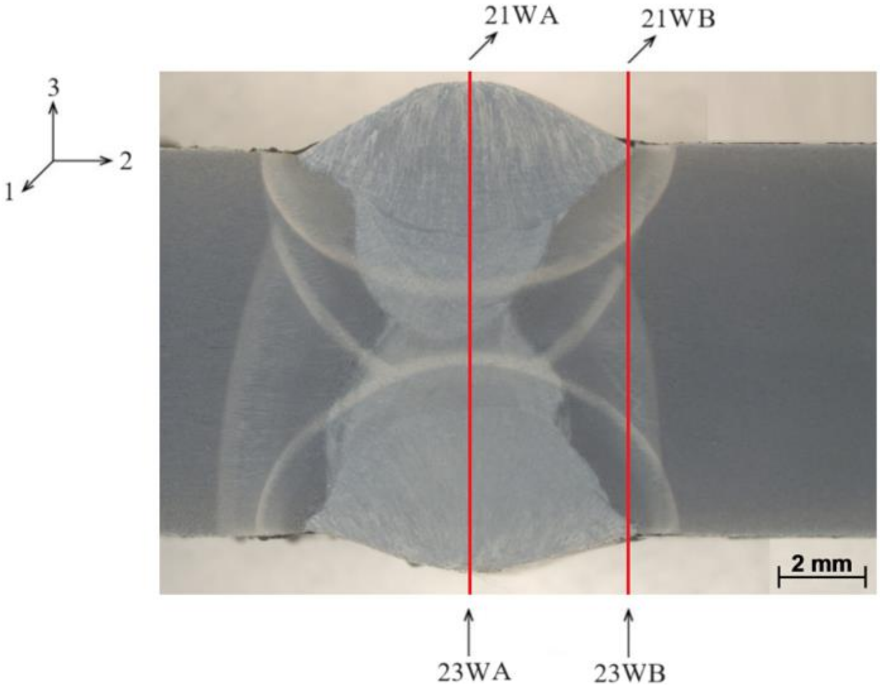

Figure 5. *Notch orientation of TPB specimens used for fatigue crack propagation tests for welded joints of S1300Q*

The locations of the notches varied throughout the tests; thus, the crack propagation provided a comprehensive understanding of the behavior of the welded joints. The control mode used during the tests was load reduction (pre-crack) or constant load amplitude (crack propagation) with a stress ratio of R = 0.1 and a sinusoidal wave form. All tests were performed in a laboratory environment at room temperature. At the beginning of the tests, the load frequency was f = 20 Hz, which was reduced to f = 5 Hz in the final phase. To ensure proper comparability of the results, the specimen preparation was uniform in all cases and the nominal value of the characteristic specimen size (W), which is relevant for the tests, was the same for each orientation.

After the tests, the crack size – number of cycle (a-N) curves were drawn from the recorded data *(Figures 6–9)*, and the kinetic diagrams of fatigue crack growth were determined using the a-N curves *(Figures 10–13)*.

Afterwards, the values of the Paris-Erdogan constant (C) and the exponent (n) of the Paris-Erdogan relation (Paris et al., 1963) were determined – from the kinetic diagrams using the method of least squares – with the correlation indexes and with the values of the fatigue fracture toughness (ΔK_{fc}). The determined n, C and ΔK_{fc} values can be seen in *Table 8* and *Table 9*. In *Table 9*, and in the followings, the designation undermatching (9) refers to the S1300Q-Böhler Union X96 and the designation undermatching (11) refers to the S1300Q-Böhler alform 1100 L-MC base material/filler material combination.

To evaluate the results, the data obtained in each test group (n and ΔK_{fc}) were considered as statistical samples and – where it was possible due to the number of samples – the similarity and dissimilarity of each sample was examined. For this purpose, a Wilcoxon test was used (Vincze, 1975), (Owen, 1973) with a two-sided significance level of ε = 0.1.

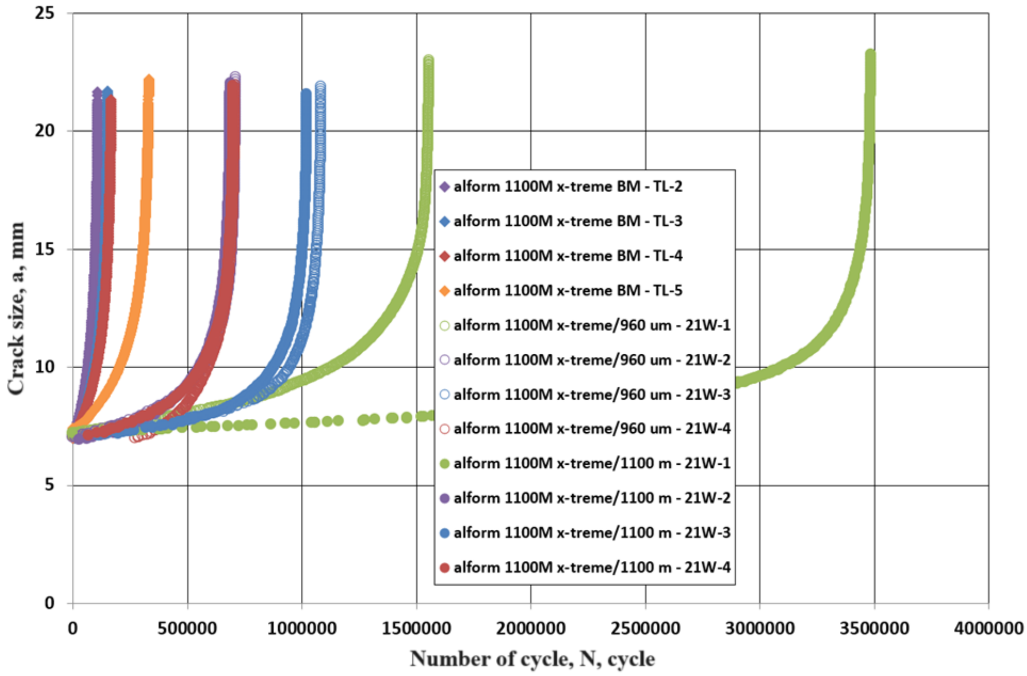

Figure 6. *a-N curves of fatigue crack propagation rate tests on S1100M base material in T-L and welded joints in 21 orientations*

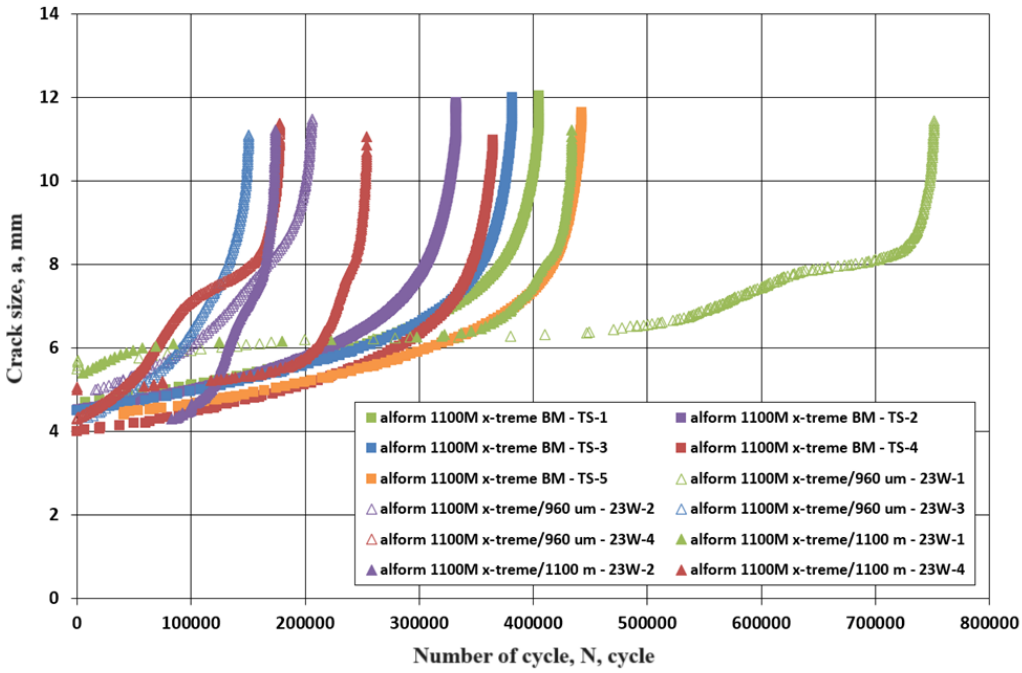

Figure 7. *a-N curves of fatigue crack propagation rate tests on S1100M base material in T-S and welded joints in 23 orientations*

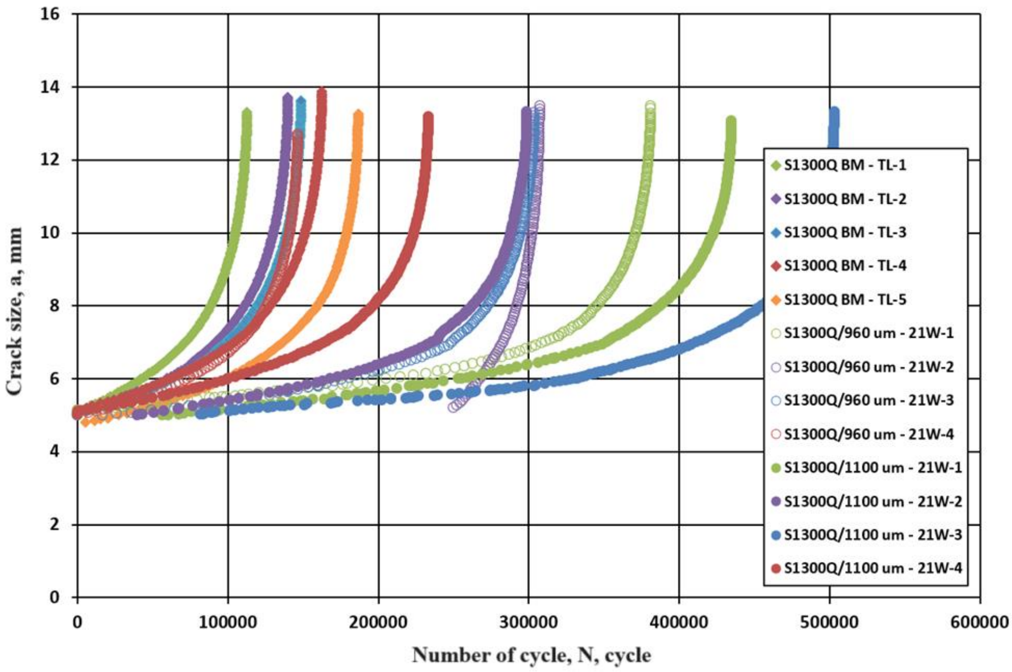

Figure 8. *a-N curves of fatigue crack propagation rate tests on S1300Q base material in T-L and welded joints in 21 orientations*

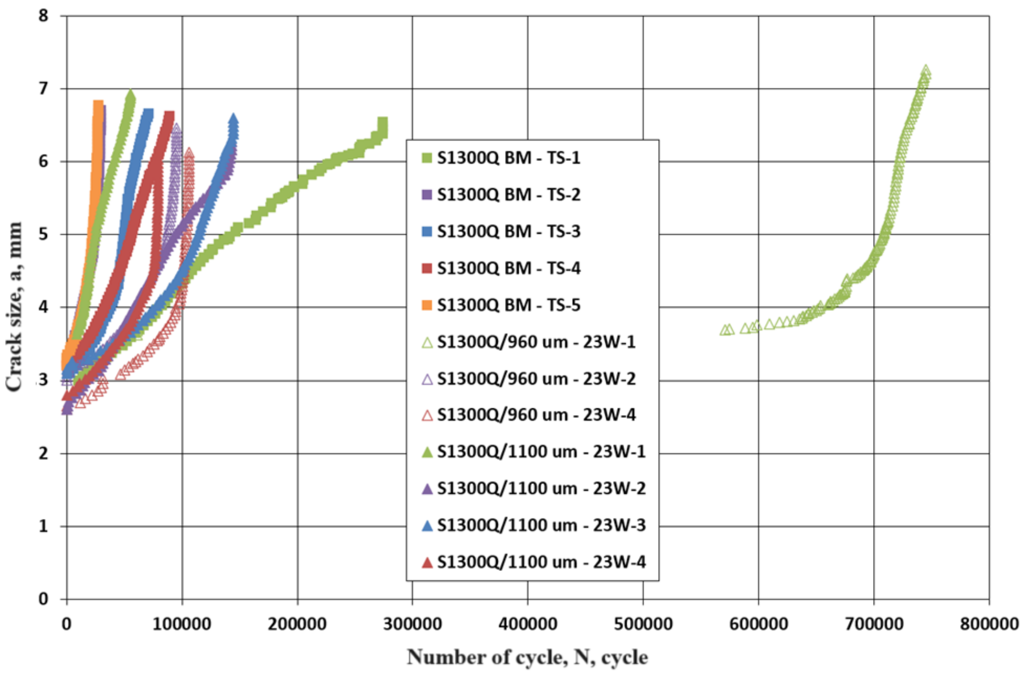

Figure 9. *a-N curves of fatigue crack propagation rate tests on S1300Q base material in T-S and welded joints in 23 orientations*

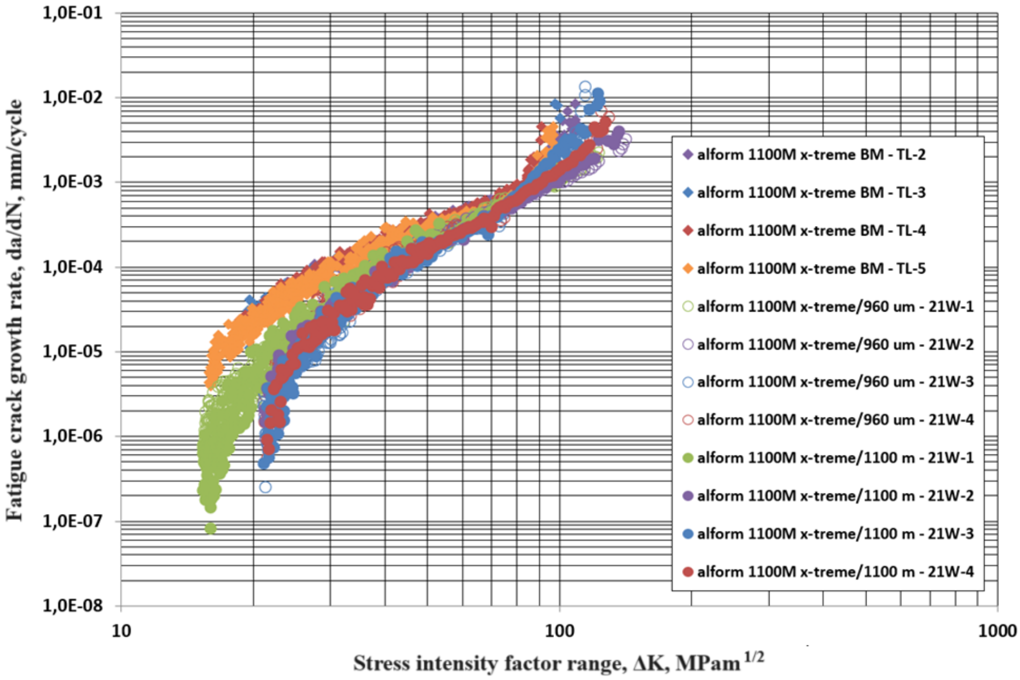

Figure 10. *da/dN-ΔK curves of fatigue crack propagation rate tests on S1100M base material in T-L and welded joints in 21 orientations*

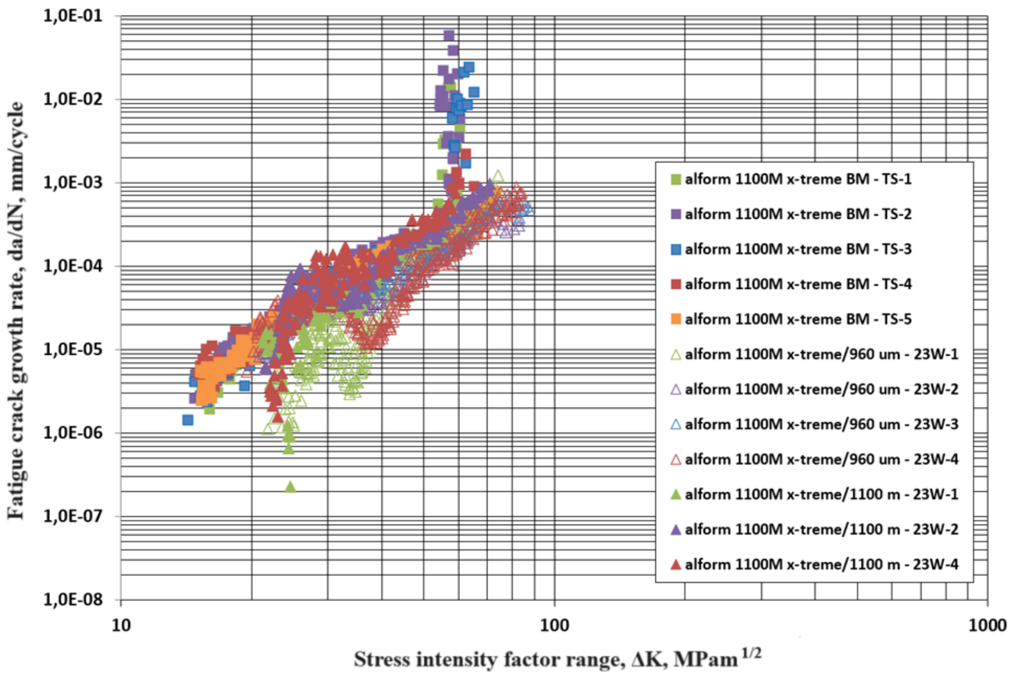

Figure 11. *da/dN-ΔK curves of fatigue crack propagation rate tests on S1100M base material in T-S and welded joints in 23 orientations*

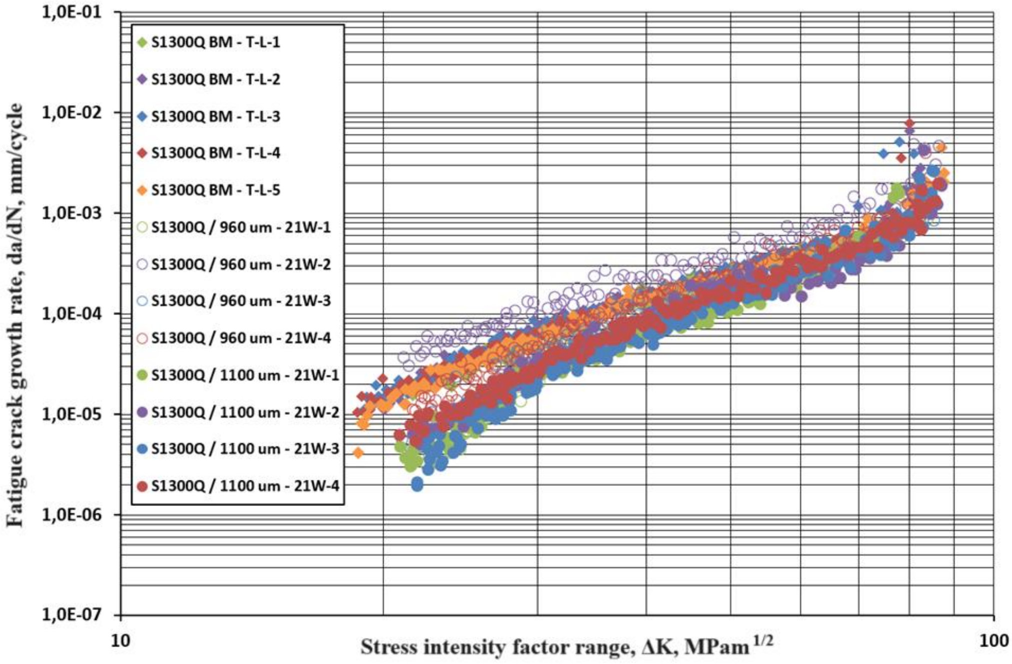

Figure 12. *da/dN-ΔK curves of fatigue crack propagation rate tests on S1300Q base material in T-L and welded joints in 21 orientations*

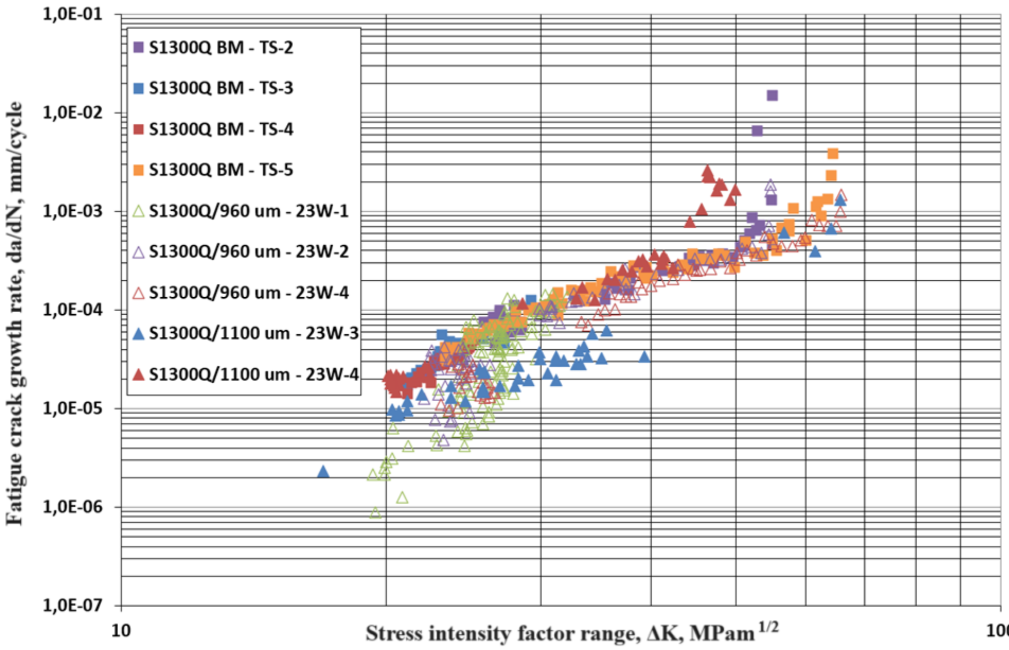

Figure 13. *da/dN-ΔK curves of fatigue crack propagation rate tests on S1300Q base material in T-S and welded joints in 23 orientations*

***Table 8.** Results of fatigue crack growth rate tests on S1100M steel and its welded joints*

Specimen ID	Location	Orientation	n	C	Correlation coefficient	ΔK_{fc}
			[mm/cycle, MPam$^{1/2}$]		[–]	[MPam$^{1/2}$]
Alform 1100M x-treme base material, T-L orientation						
A1	TL-1	T-L	no result (static failure)			
A2	TL-2		2.379	2.80E-08	0.9889	108
A3	TL-3		2.283	3.78E-08	0.9846	104
A4	TL-4		2.444	2.25E-08	0.9863	91
A5	TL-5		2.66	7.84E-09	0.9713	97
Alform 1100M x-treme base material, T-S orientation						
A6	TS-1	T-S	3.481	2.98E-10	0.9854	60
A7	TS-2		3.222	8.23E-10	0.977	61
A8	TS-3		3.457	3.48E-10	0.9862	65
A9	TS-4		3.108	1.13E-09	0.9807	66
A10	TS-5		3.136	1.04E-09	0.9856	73
Welded joint, Union X96 filler material (undermatching), 21 orientation						
C1	21W-1	21WC	3.704	7.62E-11	0.9846	123
C2	21W-2	21WC	3.161	6.10E-10	0.9844	141
C3	21W-3	21WA	3.631	9.52E-11	0.9779	115
C4	21W-4	21WB	3.363	2.97E-10	0.9815	129
Welded joint, alform 1100 L-MC filler material (matching), 21 orientation						
D1	21W-1	21WC	3.05	1.11E-09	0.9856	115
D2	21W-2	21WB	3.059	9.02E-10	0.9959	137
D3	21W-3	21WA	3.573	1.31E-10	0.9892	123
D4	21W-4	21WB	3.413	2.26E-10	0.9920	127
Welded joint, Union X96 filler material (undermatching), 23 orientation						
C5	23W-1	23WA	4.885	5.16E-13	0.9022	74
C6	23W-2	23WC	2.666	3.06E-09	0.9718	85
C7	23W-3	23WC	2.654	4.11E-09	0.9802	88
C8	23W-4	23WB	2.513	5.73E-09	0.8484	84
Welded joint, alform 1100 L-MC filler material (matching), 23 orientation						
D5	23W-1	23WA	4.211	1.58E-11	0.9680	60
D6	23W-2	23WB	2.688	6.27E-09	0.9079	71
D7	23W-3	23WA	no result (test failed)			
D8	23W-4	23WA	3.034	2.10E-09	0.9093	60

Table 9. *Results of fatigue crack growth rate tests on S1300Q steel and its welded joints*

Specimen ID	Location	Orientation	n	C	Correlation coefficient	ΔK_{fc}
			[mm/cycle, MPam$^{1/2}$]		[–]	[MPam$^{1/2}$]
S1300Q base material, T-L orientation						
B1	TL-1	T-L	2.876	3.14E-09	0.9938	85
B2	TL-2		2.860	3.57E-09	0.9906	82
B3	TL-3		2.900	3.13E-09	0.9914	81
B4	TL-4		2.852	3.49E-09	0.9921	82
B5	TL-5		2.932	2.50E-09	0.9928	88
S1300Q base material, T-S orientation						
B6	TS-1	T-S	not assessable (limited data, unstable data series)			
B7	TS-2		2.953	4.14E-09	0.9736	55
B8	TS-3		not assessable (limited data)			
B9	TS-4		not assessable (limited data)			
B10	TS-5		3.024	3.32E-09	0.9750	64
Welded joint X96 filler material [undermatching (9)], 21 orientation						
E1	21W-1	21WB	4.289	9.52E-12	0.9711	84
E2	21W-2	21WB	2.678	1.17E-08	0.9872	86
E3	21W-3	21WB	3.542	1.76E-10	0.9714	86
E4	21W-4	21WA	3.288	6.16E-10	0.9854	84
Welded joint alform 1100 L-MC filler material [undermatching (11)], 21 orientation						
F1	21W-1	21WB	3.787	4.87E-11	0.9885	79
F2	21W-2	21WB	3.398	2.48E-10	0.9766	87
F3	21W-3	21WB	3.880	3.49E-11	0.9873	86
F4	21W-4	21WA	3.526	1.66E-10	0.9927	86
Welded joint Union X96 filler material [undermatching (9)], 23 orientation						
E5	23W-1	23WA	8.873	7.40E-18	0.8120	32
E6	23W-2	23WA	3.705	2.37E-10	0.9632	55
E7	23W-3	23WB	no result (test failed)			
E8	23W-4	23WB	4.222	2.35E-11	0.9745	66
Welded joint alform 1100 L-MC filler material [undermatching (11)], 23 orientation						
F5	23W-1	23WB	not assessable (limited data, unstable data series)			
F6	23W-2	23WB	not assessable (crack stopping)			
F7	23W-3	23WB	3.321	3.57E-10	0.9373	66
F8	23W-4	23WB	4.997	4.75E-12	0.9747	50

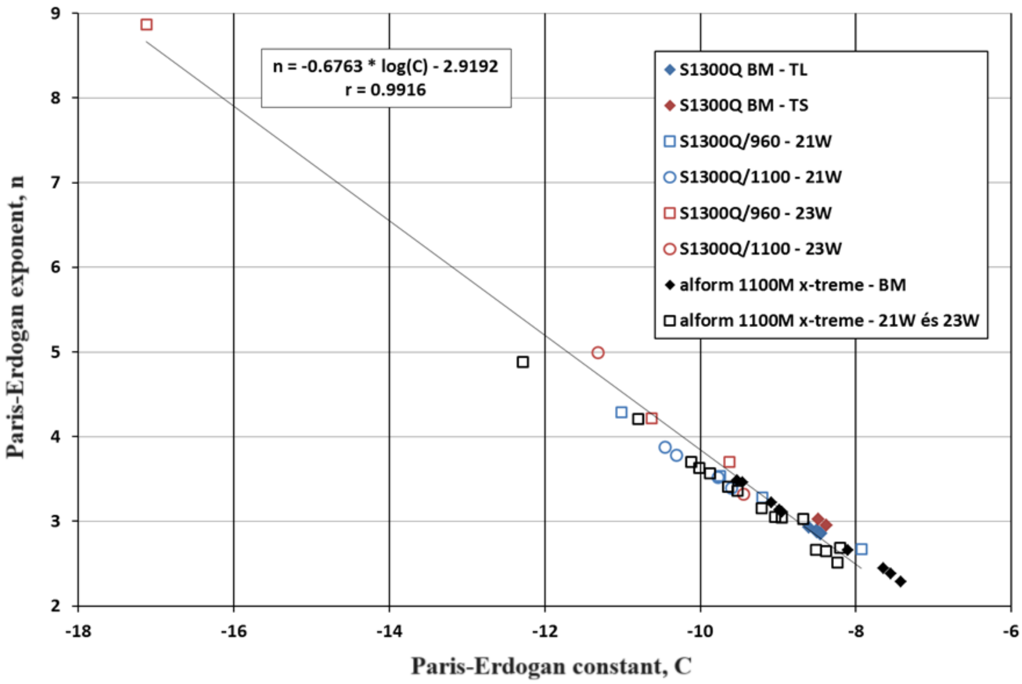

Figure 14. *Connection between the two parameters of Paris-Erdogan equation for the investigated base materials and their welded joints (calculated from S1300Q data only)*

Both the correlation coefficient values shown in *Table 8* and *Table 9* and the relationship just as the correlation coefficients in *Figure 14* show reliable and reproducible tests. It can also be concluded that the results of the tests carried out on the investigated two different steel grades are in good correspondence with each other.

To evaluate the results, the data obtained in each test group (n and ΔK_{fc}) were considered as statistical samples and – where it was possible due to the number of samples – the similarity and dissimilarity of each sample was examined. For this purpose, a Wilcoxon test was used (Vincze, 1975), (Owen, 1973) with a two-sided significance level of $\varepsilon = 0.1$.

First, the different material orientations (T-L and T-S) were examined, and it was found that the difference was significant, and the samples should be treated separately. Secondly, for the welded joints of S1100M, the undermatching and matching combinations by orientation (21W and 23W) were analyzed and it was found that the differences are not significant – except for the ΔK_{fc} samples of the 23W orientation – and the samples can be grouped into a single sample – except for the ΔK_{fc} samples of the 23W orientation. With this knowledge, it was also examined whether the samples grouped by welded joint orientation (21W and 23W) could be considered similar or not. The result obtained that these samples are significantly different in all cases. The individual and merged samples and their statistical characteristics are summarized in *Table 10*, where those samples that were not significantly different, i.e. which were then merged, are shown in italics. The standard deviation coefficient values in the table, compared to those in (Gáspár et al., 2013) and (Mobark, 2020), are favorable (below 0.3), except for n samples of the 23W orientation, whether they are individual or merged samples. This finding further strengthens the statement regarding the reliability and reproducibility of the tests.

Table 10. *Results of the fatigue crack growth rate tests on S1100M steel and their statistical design and characteristics*

Sample	Orientation / mismatching	Element number of the sample	Average value	Standard deviation	Standard deviation coefficient
n	T-L	4	2.442	0.160	0.0655
n	T-S	5	3.281	0.177	0.0540
ΔK_{fc}	T-L	4	100.0	7.61	0.08
ΔK_{fc}	T-S	5	65.1	5.08	0.08
n	*21W / undermatching*	*4*	*3.465*	*0.250*	*0.0722*
n	*21W / matching*	*4*	*3.274*	*0.261*	*0.0799*
ΔK_{fc}	*21W / undermatching*	*4*	*127.0*	*11.21*	*0.09*
ΔK_{fc}	*21W / matching*	*4*	*125.5*	*9.06*	*0.07*
n	21W / undermatching és 21W / matching	8	3.369	0.258	0.0765
ΔK_{fc}	21W / undermatching és 21W / matching	8	126.2	9.47	0.08
n	*23W / undermatching*	*4*	*3.180*	*1.139*	*0.3583*
n	*23W / matching*	*3*	*3.311*	*0.798*	*0.2411*
ΔK_{fc}	23W / undermatching	4	82.6	5.99	0.07
ΔK_{fc}	23W / matching	3	63.6	6.18	0.10
n	23W / undermatching és 23W / matching	7	3.24	0.93	0.2876

In case of S1300Q, the different base material orientations (T-L and T-S) were firstly examined, and it was found that the difference was significant, and the samples should be treated separately. Subsequently, for the 21W welded joint orientation, the two undermatching combinations [undermatching (9) és undermatching (11)] were analyzed and it was found that the differences are not significant – for either the n or ΔK_{fc} samples – and the samples can be grouped into a single sample. The same analysis could not be performed for the 23W welded joint orientation due to limited numbers of samples. In a third step, assuming that the 23W orientation would lead to the same result as the 21W orientation, it was also examined whether or not the samples grouped by weld orientation (21W and 23W) could be considered as similar. The result was that these samples would be significantly different in all cases.

The individual and merged samples and their statistical characteristics are summarized in *Table 11*, where those samples that were not significantly different, i.e., those that were then merged, are shown in italics.

By comparing the standard deviation coefficient values in the table with those in (Lukács et al., 2012) and (Balogh et al., 2015), it can be seen that they are favorable (below 0.3), except for the n samples of the 23W/undermatching (11) pairing, for both the individual and merged samples. Thus, this finding further confirms the statement on the reliability and reproducibility of the tests.

Table 11. *Results of the fatigue crack growth rate tests on S1300Q steel and their statistical design and characteristics*

Sample	Orientation / mismatching	Element number of the sample	Average value	Standard deviation	Standard deviation coefficient
n	T-L	5	2.884	0.032	0.0113
n	T-S	2	2.989	0.050	0.0168
ΔK_{fc}	T-L	5	83.7	2.73	0.03
ΔK_{fc}	T-S	2	59.8	6.65	0.01
n	*21W / undermatching (9)*	*4*	*3.449*	*0.667*	*0.1934*
n	*21W / undermatching (11)*	*4*	*3.648*	*0.224*	*0.0614*
ΔK_{fc}	*21W / undermatching (9)*	*4*	*85.1*	*1.16*	*0.01*
ΔK_{fc}	*21W / undermatching (11)*	*4*	*84.4*	*3.97*	*0.05*
n	21W / undermatching (9) és 21W / undermatching (11)	8	3.55	0.47	0.1332
ΔK_{fc}	21W / undermatching (9) és 21W / undermatching (11)	8	84.8	2.73	0.03
n	23W / undermatching (9)	2	3.964	0.366	0.0922
n	23W / undermatching (11)	2	4.159	1.185	0.2850
ΔK_{fc}	23W / undermatching (9)	2	60.3	7.84	0.13
ΔK_{fc}	23W / undermatching (11)	2	57.8	11.09	0.19

4. Summary

Based on the results of the FCP tests on the S1100M and S1300Q materials, the reliability and reproducibility of the FCP tests performed with a statistical approach, both from the individual results and from the statistical sample data, can be considered as good.

The resistance of the tested materials to FCP is significantly different in the rolling direction and in the thickness direction, the materials are more sensitive to crack propagation in the thickness direction. The significant difference is demonstrated by both the Paris–Erdogan exponent and the fatigue fracture toughness values.

The FCP resistance of the welded joints is different than that of the base materials, and the difference is greater in the thickness direction than in the rolling direction. The resistance to FCP of welded joints produced with two different filler metals is not significantly different in the rolling direction. For S1100M, there is no difference in the thickness direction either. For S1300Q, however, there is insufficient data to conclude this type of conclusion in the thickness direction. For both tested materials, it can be observed that the resistance of welded joints to FCP in the rolling direction and in the thickness direction, is significantly different, the cracks that propagate in the thickness direction behaving differently from the cracks that propagate in the rolling direction. The reason for this is that cracks propagated in the thickness direction pass through more HAZs than cracks propagated in the rolling direction. Welded joints are more susceptible to thickness direction cracks.

For S1100M, the fatigue fracture toughness of welded joints typically exceeds that of the base material. In the case of S1300Q, there is no significant difference between the fatigue fracture toughness of the base material and that of the welded joints. In conclusion, it can also be noted that the characteristics of the tests carried out on the two investigated base materials (despite their different chemical compositions and production methods) and their welded joints are in good correlation.

References

[1] Lahtinen, T., Vilaca, P., Peura, P. & Mehtonen, S. (2019). MAG welding tests of modern high strength steels with minimum yield strength of 700 MPa. *Appleid Sciences*, 9, p. 1031. **https://doi.org/10.3390/app9051031**

[2] Raabe, D. (2023). Materials Science behind Sustainable Metals and Alloys. *Chemical Reviews*, 123(5), pp. 2436–2608, **https://doi.org/10.1021/acs.chemrev.2c00799**

[3] Jha, R. N., Dutta, K. & Ray, K. K. (2012). Effect of tempering on mechanical properties of V-added AISI 4335 steel. *ISIJ International*, 50(4), pp. 607–612.

[4] Shi, Z. M., Liu, K. & Wang, M. Q. (2012). Effect of tensile deformation of austenite on the morphology and strength of lath martensite. *Metals and Materials International*, 18(2), pp. 317–320. **https://doi.org/10.1007/s12540-012-2015-5**

[5] Weglowski, M. St., Zeman, M. & Lomozik, M. (2013). Physical Simulation of Weldability of Weldox 1300 Steel. *Material Science Forum*, 762, pp. 551–555. **https://doi.org/10.4028/www.scientific.net/MSF.762.551**

[6] Weglowski M. St. & Zeman, M. (2014). Prevention of cold cracking in ultra-high strength steel Weldox 1300. *Archives of Civil and Mechanical Engineering*, 14(3), pp. 417–424. **https://doi.org/10.1016/j.acme.2013.10.010**

[7] Tümer, M., Pixner, F. & Enzinger, N. (2021). Residual Stresses, Microstructure, and Mechanical Properties of Electron Beam Welded Thick S1100 Steel. *Journal of Materials Engineering and Performance*, 31, pp. 2136–2146. **https://doi.org/10.1007/s11665-021-06348-1**

[8] Chen, M.-T., Cai, A., Pandey, M., Shen, C., Zhang, Y. & Hu, L. (2023). Mechanical properties of high strength steels and weld metals at arctic low temperatures. *Thin-Walled Structures*, 185, p. 110543, **https://doi.org/10.1016/j.tws.2023.110543**

[9] Yu, J., Ziehl, P., Zárate, B. & Caicedu, J. (2011). Prediction of fatigue crack growth in steel bridge components using acoustic emission. *Journal of Constructional Steel Research*, 67(8), pp. 1254–1260. **https://doi.org/10.1016/j.jcsr.2011.03.005**

[10] Zhang, Y., Wang, S., Xu, G., Wang, G., & Zhao, M. H. (2022). Effect of microstructure on fatigue-crack propagation of 18CrNiMo7-6 high-strength steel. *International Journal of Fatigue*, 163, p. 107027. **https://doi.org/10.1016/j.ijfatigue.2022.107027**

[11] Li, H. F., Zhang, P. & Zhang, Z. F. A new fatigue crack growth mechanism of high-strength steels. *Materials Science and Engineering: A*, 840, p. 142969. **https://doi.org/10.1016/j.msea.2022.142969**

[12] Lukács, J., Nagy, Gy., Harmati, I., Fótos, R. K. & Koncsik Zs. K. L. (2012). *Szemelvények a mérnöki szerkezetek integritása témaköréből*. Miskolci Egyetem.

[13] Koncsik, Zs. (2021). Szerkezetintegritási kutatások az Innovatív Anyagtechnológiák Tudományos Műhelyben. *Multidiszciplináris Tudományok*, 11(2), pp. 372–379. **https://doi.org/10.35925/j.multi.2021.2.49**

[14] Koncsik, Zs. (2022). Szerkezetintegritási esettanulmányok. In: Zs. Koncsik, J. Lukács (eds.). *Kutatási eredmények a Miskolci Egyetem Gépészmérnöki és Informatikai Karának Anyag-szerkezettani és Anyagtechnológiai Intézetében*. Miskolci Egyetem, 1st ed., pp. 133–144.

[15] Weglowski, M. St. & Zeman, M. (2014). Prevention of cold cracking in ultra-high strength steel Weldox 1300. *Archives of Civil and Mechanical Engineering*, 14(3), pp. 417–424. **https://doi.org/10.1016/j.acme.2013.10.010**

[16] Voestalpine (2024). *Alform – High-strength and ultra high-strength thermomechanically rolled fine-grained steels*. 01, 1–23.

[17] Mobark, H. F. H. (2020). *Fatigue strength and fatigue crack propagation design curves for high strength steel structural elements*. PhD theses, Miskolc, pp. 67–82.

[18] ASTM E1823-21. (2021). Standard Terminology Relating to Fatigue and Fracture Testing, ASTM International.

[19] Paris, P., & Erdogan, F. (1963). A Critical Analysis of Crack Propagation llaws. *Journal of Basic Engineering*, *Transactions of the ASME*, pp. 528–534.

[20] Vincze, I. (1975). *Matematikai statisztika ipari alkalmazásokkal*. Műszaki Könyvkiadó, Budapest.

[21] Owen, D. B. (1973). Handbook of statistical tables. Vychislitel'nyjj Centr AN SSSR, Moskva

[22] Gáspár, M., & Balogh A. (2013). GMAW experiments for advanced (Q+T) high strength steels. *Production Processes and Systems,* 6 (1), pp. 9–24.

[23] Balogh, A., Lukács, J., & Török, I. (2015). Hegeszthetőség és a hegesztett kötések tulajdonságai. Kutatások járműipari acél és alumínium ötvözet anyagokon, Miskolci Egyetem, pp, 11–41., 202–209.